Evolution of the Fermi Surface and Quasiparticle Renormalization through a van Hove Singularity in $Sr_{2-y}La_yRuO_4$

K. M. Shen,[1,2,*] N. Kikugawa,[3,†] C. Bergemann,[4] L. Balicas,[5] F. Baumberger,[1,3] W. Meevasana,[1] N. J. C. Ingle,[1,2] Y. Maeno,[6,7] Z.-X. Shen,[1] and A. P. Mackenzie[3]

[1]*Departments of Applied Physics, Physics, and Stanford Synchrotron Radiation Laboratory, Stanford University, Stanford, California 94305, USA*

[2]*Department of Physics and Astronomy, University of British Columbia, Vancouver, B.C., V6T 1Z4, Canada*

[3]*School of Physics & Astronomy and Scottish Universities Physics Alliance, University of St. Andrews, North Haugh, St. Andrews KY16 9SS, United Kingdom*

[4]*Cavendish Laboratory, University of Cambridge, J. J. Thomson Avenue, Cambridge CB3 OHE, United Kingdom*

[5]*National High Magnetic Field Laboratory, Florida State University, Tallahassee Florida 32306, USA*

[6]*International Innovation Center, Kyoto University, Kyoto 606-8501, Japan*

[7]*Department of Physics, Graduate School of Science, Kyoto University, Kyoto 606-8502, Japan*

(Received 26 March 2007; published 29 October 2007)

We employ a combination of chemical substitution and angle resolved photoemission spectroscopy to prove that the Fermi level in the γ band of $Sr_{2-y}La_yRuO_4$ can be made to traverse a van Hove singularity. Remarkably, the large mass renormalization has little dependence on either $\mathbf{k}$ or doping. By combining the results from photoemission with thermodynamic measurements on the same batches of crystals, we deduce a parametrization of the full many-body quasiparticle dispersion in Sr_2RuO_4 which extends from the Fermi level to approximately 20 meV above it.

DOI: 10.1103/PhysRevLett.99.187001 PACS numbers: 74.20.Rp, 74.25.Jb, 74.72.−h, 79.60.−i

The layered perovskite ruthenate Sr_2RuO_4 has attracted considerable attention and interest, stimulated initially by its unconventional superconductivity [1,2]. There is now a considerable body of evidence that it is a spin triplet superconductor with a time-reversal symmetry breaking ground state [2–5] and that the metal from which the superconductivity condenses is a nearly two-dimensional Fermi liquid with a substantial mass enhancement [6]. The electronic structure near the Fermi level consists of two Fermi surface sheets (α and β) having strong Ru $d_{xz,yz}$ character and a third, γ, based on the in-plane Ru d_{xy} orbital.

The comprehensive knowledge that has been acquired about the Fermi liquid properties of Sr_2RuO_4 is unprecedented for a transition metal oxide, making it an ideal material in which to address a deeper layer of important questions, for example the origin of the mass enhancement and its relationship to the microscopic mechanism of the superconductivity. Recently, a new route to probing this was opened by the observation that the heterovalent substitution of La^{3+} for Sr^{2+} to form $Sr_{2-y}La_yRuO_4$ produces a rigid-band shift of the Fermi level for low y [7]. The limit on those experiments was the window for observing a de Haas–van Alphen (dHvA) signal, which is exponentially suppressed by disorder scattering, and not the solubility limit of La^{3+} in Sr_2RuO_4. In fact, much higher substitution levels of up to $y = 0.27$ have been achieved, raising the possibility that the Fermi level can be forced to traverse a van Hove singularity (vHS) in the γ band. This issue is of great interest, since strong electronic renormalization and scattering of quasiparticles could occur near such a singularity in the density of states. For instance, it has even been postulated that some of the unusual physical properties observed in the cuprate superconductors might be as a result of the vicinity of a vHS to E_F at $\mathbf{k} = (\pi, 0)$. In this Letter we report the results of a careful set of experiments which prove conclusively that the mass renormalization remains remarkably independent of both $\mathbf{k}$ and doping as the vHS traverses E_F.

In principle, angle resolved photoemission spectroscopy (ARPES) is ideally suited to this experiment, since it is not subject to the same purity restrictions as dHvA. However, since it is highly surface-sensitive there is always the concern that some of the information that it yields is a property of the surface rather than the bulk electronic structure. This issue has been of particular significance to ARPES studies of Sr_2RuO_4, as discussed in Refs. [2,8,9]. For this reason we set ourselves the more ambitious goal of performing a detailed comparison of ARPES with bulk measurements of the Fermi surface topography and excitation spectrum. The ARPES work was performed with a Gammadata VUV5000 He-discharge lamp, monochromator, and a SES2002 electron analyzer, at a base temperature of 10 K and a pressure of better than 4×10^{-11} torr. All data shown in this Letter were collected using He II photons (40.81 eV) on samples cleaved at 200 K, in order to suppress the surface-related features discussed in Refs. [8,9]. A new generation of dHvA measurements was also performed in the world's highest steady magnetic field of 45 T using using a Cu-Be torque magnetometer with capacitive readout, at temperatures between 0.04 and 0.9 K.

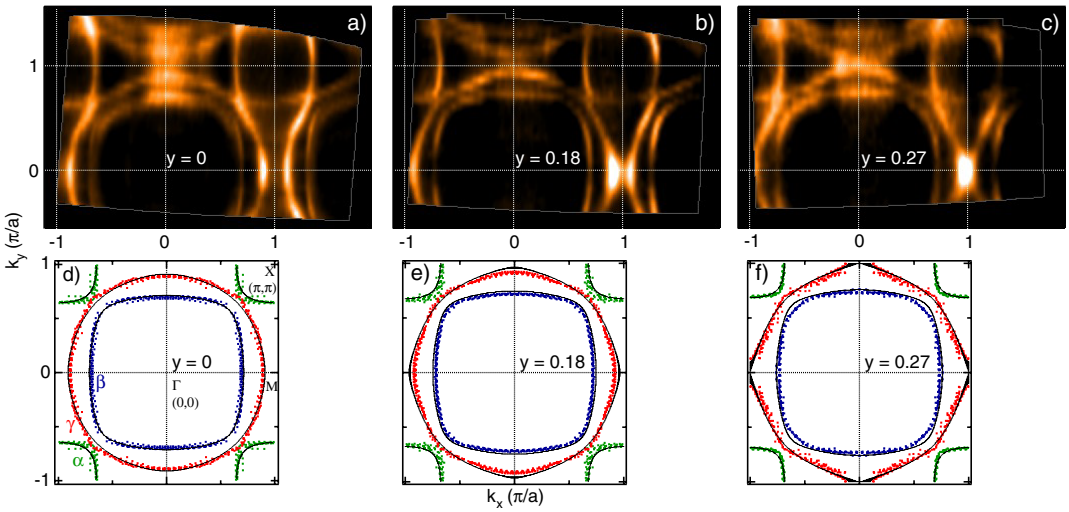

FIG. 1 (color online). (a)–(c) Raw ARPES spectral intensity k-space maps for $Sr_{2-y}La_yRuO_4$, using an integration window of $E_F \pm 5$ meV, and an energy resolution of 16 meV, each generated from approximately 10^4 energy distribution curves (EDCs). Data have not been symmetrized. (d)–(f) Precise Fermi surface crossings in the 2D projected Brillouin zone determined by fitting the intensity maxima of cuts running roughly perpendicular to the Fermi surfaces, set against the predictions of the tight-binding rigid-band shift model described in the text (black solid lines). Fermi surface sheets are labeled in (d).

In Figs. 1(a)–1(c) we show raw ARPES intensity maps at the Fermi energy for three crystals with $y = 0$, 0.18 and 0.27. The α, β, and γ Fermi surface sheets are clearly visible in each case and labeled in Fig. 1(a). The most important changes, those to the γ sheet, are immediately visible in the raw data. At $y = 0$ the γ sheet obviously does not touch the zone boundary, at $y = 0.18$ the FS seems to nearly touch, while at $y = 0.27$ the γ sheet does appear to cross the zone boundary near the M point, as illustrated in greater detail in Fig. 2. The striking results of using a more sophisticated algorithm to obtain the Fermi wave vectors, $\mathbf{k}_F$s, for each doping level are shown in Figs. 3(d)–3(f), confirming the change of the γ sheet from electronlike to holelike between $y = 0.18$ and 0.27.

As a first reference against which to compare the data, we can make use of a simple model based on the precise knowledge which exists of the Fermi surface at $y = 0$ [6,7,10]. That Fermi surface can be fitted well with the simple tight-binding dispersions summarized in Table 1 of Ref. [6]. If one postulates that the only effect of a La^{3+} substitution is to shift the chemical potential rigidly through these bands by introducing exactly one electron per La to them, one obtains (with no additional fitting parameters) the solid lines shown in Figs. 1(d)–1(f). This good agreement is significant, because there is no *a priori* reason that the common "rigid-band shift" assumption should hold in this situation. Luttinger's theorem states that the volume enclosed within all Fermi surfaces is equal to the total number of occupied valence electrons, even in the presence of correlations. However, it is known theoretically that in multiband systems, electronic correlations can shift electrons from one band to another, so that the relative volumes of each individual FS sheet need not remain constant, only the total volume [11–14]. The data shown in Figs. 1(d)–1(f) prove that any such interband shift of carriers due to La doping is a small effect in $Sr_{2-y}La_yRuO_4$.

To check explicitly for a vHS crossing, we performed sets of direct E vs $\mathbf{k}$ measurements which cut through the M point along the Γ-M-Γ high symmetry line. In Fig. 2(a) we show the γ band dispersing on either side of M, with the $\mathbf{k}_F$s on either side of the M point demonstrating an obvious electronlike topology. To find the position of the unoccupied vHS, we thermally populated states above E_F by raising the temperature to 100 K, as shown in 2(b), showing that the vHS lies approximately 14 meV above E_F. In 2(c), with $y = 0.18$, we have drawn the experimentally measured Fermi level as a thin white line, but referencing the dispersion to that of the undoped material shows that E_F has been raised by 13 meV, very nearly to the vHS. By $y = 0.27$ the Fermi level lies 19 meV above that of the undoped material, and approximately 4 meV above the top of the band. A precise extraction of the loci of quasiparticle peaks, obtained from the maxima in the ARPES energy distribution curves at a series of y values, is shown in Fig. 2(e). When the data are overlaid by the rigid-band shifts deduced from the raw data they are seen to follow the same simple cosine function (black line).

The ARPES results presented in Figs. 1 and 2 give clear evidence for a vHS crossing in $Sr_{2-y}La_yRuO_4$ for $y \sim 0.2$. One of the key aspects of this work is the ability to combine our ARPES measurements with bulk-sensitive dHvA and specific heat measurements, and band structure calculations. This allows us to crosscheck the highly direct and precise, yet surface-sensitive, ARPES measurements with a bulk Fermi surface probe (dHvA). Furthermore, we can

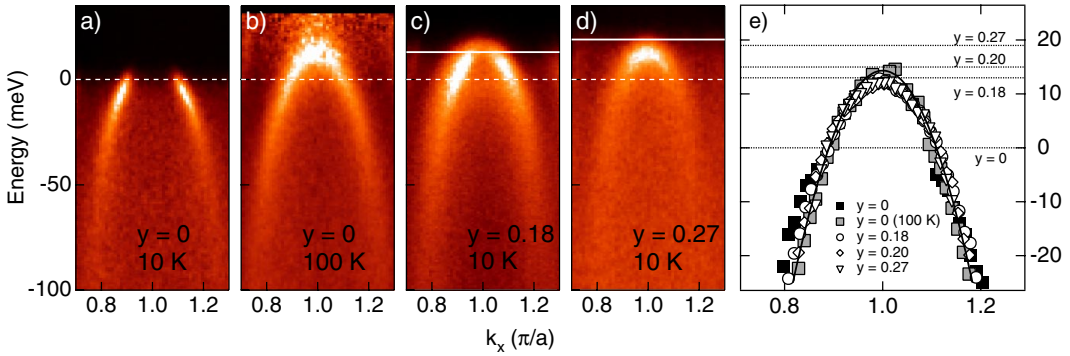

FIG. 2 (color online). Scans along the Γ-M-Γ line in the Brillouin zone for samples with $y = 0$, $y = 0.18$ and $y = 0.27$ at 10 K and $\Delta E < 8$ meV energy resolution, (a), (c), (d) and for $y = 0$ at 100 K divided by the Fermi-Dirac distribution (b). In all cases the true experimentally measured E_F (solid white line) was referenced to that of an Au target in direct electrical contact with the sample. The dotted white lines in (c) and (d) show the Fermi level for $y = 0$, to highlight the magnitude of the doping-induced shift.

also verify that these probes yield an electronic structure consistent with one expected from measuring bulk thermodynamic properties (specific heat). In Fig. 3(a) we present the direct comparison of Fermi surface topography measurements by dHvA and ARPES across a range of cation substituted single crystals. By using the 45 T hybrid magnet at the U. S. National High Magnetic Field Laboratory in Tallahassee, we were able to measure all three main dHvA frequencies out to $y = 0.06$, and the smallest α frequency all the way to $y = 0.1$.

Our findings have significant implications for the physics of many-body renormalization in Sr_2RuO_4. If this renormalization is dominated by coupling to a sharp mode, it results in a kink in the dispersion at a characteristic energy associated with that mode. If, on the other hand, it is dominated by coupling to a continuum of electron-hole excitations, renormalization of the whole band is possible. For this to occur, the source of the renormalization must be local in real space since its effects are spread out over all $\mathbf{k}$. A notable example is the simplified on-site repulsion U employed to partially account for correlations in modern electronic structure calculations. The extent of renormalization can also be linked to the magnitude of the bare density of states, so naively one might expect a feedback effect in which the correlation-induced enhancement factor is increased near the vHS. Several features of our data suggest that, perhaps surprisingly, the renormalization of the γ band is dominated by a global band renormalization. The data from across the range of La dopings that we have employed fall onto a single cosine, even on the most crucial Γ-M-Γ cut through the vHS, and has a total bandwidth approximately a factor of 6 smaller than the LDA prediction, in agreement, within experimental error, with the dHvA-measured mass renormalization at $y = 0$ of $m^*/m_{\text{band}} = 5.5$ [2]. It can also be tracked over a wide range of $\mathbf{k}$ (at least 20% of the Brillouin zone dimension), confirming that the source of the renormalization is highly local in real space.

The data in Fig. 2(e) are from a restricted cut in the Brillouin zone, and do not, in isolation, allow us to draw firm conclusions about the renormalized band shape for the remainder of the γ band or that of the α and β bands. Indeed, attempting to do this using ARPES would be rather complex [15]. However, if local correlations dominate the renormalization in the γ band, it is highly plausible that the same considerations apply elsewhere in the Brillouin zone as well.

We are able to investigate this issue by assuming that the whole-bandwidth renormalization applies throughout the

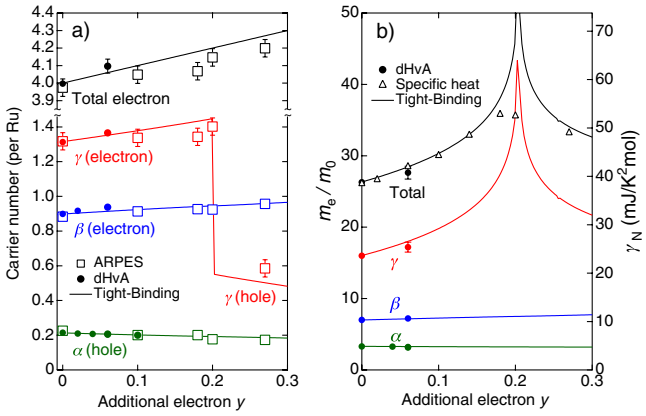

FIG. 3 (color online). dHvA (closed circles) and ARPES (open squares) data for the carrier number of each of the three Fermi surface sheets as a function of y. The data from the two techniques is in excellent agreement where there is overlap (at $y = 0$ and, for the α pocket, at $y = 0.1$). (b) The dHvA effective masses (closed circles) and electronic specific heat coefficient γ_N (defined as C_p/T at 500 mK, with C_p denoting the specific heat at constant pressure; open triangles) plotted as a function of y. In a quasi-two-dimensional material, the sum of the dHvA masses should be proportional to the electronic specific heat, and as seen from the graph, the agreement is excellent both at $y = 0$ and $y = 0.06$. In all three panels the solid lines are calculated using the model discussed in the text.

Brillouin zone, and using the mass renormalizations measured by dHvA at $y = 0$ as global compression factors (details given below in [16]). Treating these globally renormalized bands as rigid, we calculate the y dependence of the band filling and electronic specific heat, and compare them (solid lines) with the results of direct measurement by ARPES, dHvA, and specific heat [10] in Figs. 3(a) and 3(b). The agreement between prediction and measurement is good across the entire range, except very near the van Hove singularity. A possible reason for the discrepancy here is disorder broadening. Although La^{3+} is a weak potential scatterer with a phase shift of $\delta_0 \sim \pi/12$ [7], $y = 0.2$ still corresponds to a scattering rate of a few meV, enough to smear out the peak in the density of states shown in Fig. 3(b). This may also explain the fact that, contrary to intuition, the effects on the physical properties of traversing a vHS are found to be mild. Both the specific heat and resistivity develop non-Fermi liquid exponents for the concentration ($y = 0.20$) closest to the crossing point, but these are seen only at low temperatures, and there is no evidence for the onset of long-range order [10].

The deduction of the renormalized band dispersion [16] is arguably the most significant result of this paper. To within errors that can be judged by inspection of Fig. 3(b), it gives a good representation of the full many-body quasiparticle dispersion of Sr_2RuO_4 for the energy range E_F to approximately $E_F \pm 20$ meV, and it seems plausible that it would apply over a still wider range of energies. The fact that the renormalization appears to be fairly structureless does not mean that the full many-body susceptibilities will also lack structure. On the contrary, they will have a well-defined $\mathbf{k}$ and ω structure that can be calculated directly from Ref. [16]. We thus believe that our findings will form a strong foundation for future theoretical investigations of the mechanism of the unconventional superconductivity of Sr_2RuO_4. Many-body susceptibilities are, for example, a key input to calculations of spin-fluctuation mediated superconductivity [17,18]. We stress that to be able to draw this conclusion with real conviction has required us to employ a unique combination of chemical substitution, ARPES, and bulk thermodynamic measurements of dHvA and specific heat. Our work also raises interesting questions about the importance of proximity to van Hove singularities in determining the physics of this and other d-band oxides.

The authors would like to thank B. L. Brandt, R. Dunkel, T. Fujita, J. Hori, P. D. A. Mann, T. P. Murphy, E. C. Palm, Y. Shibata, and T. Suzuki for technical support and assistance. ARPES measurements at Stanford were supported by DOE contract DE-FG03-01ER45929-A001 and NSF grant DMR-0604701 and ONR N00014-98-1-0195. Work at St. Andrews was supported by an Engineering and Physical Sciences Research Council Portfolio Partnership and the Leverhulme Trust. N. K. acknowledges the Japan Society for the Promotion of Science for support. K. M. S. would like to thank NSERC, SGF, and the Killam Trusts. C. B. acknowledges the support of the Royal Society.

*Present address: LASSP, Department of Physics, Cornell University, Ithaca, NY 14853, USA.

†Present address: National Institute for Materials Science, Tsukuba 305-0047, Japan.

[1] Y. Maeno *et al.*, Nature (London) **372**, 532 (1994).
[2] For a review, see A. P. Mackenzie and Y. Maeno, Rev. Mod. Phys. **75**, 657 (2003).
[3] K. D. Nelson *et al.*, Science **306**, 1151 (2004).
[4] J. Xia *et al.*, Phys. Rev. Lett. **97**, 167002 (2006).
[5] F. Kidwingira *et al.*, Science **314**, 1267 (2006).
[6] For a review, see C. Bergemann *et al.*, Adv. Phys. **52**, 639 (2003).
[7] N. Kikugawa *et al.*, Phys. Rev. B **70**, 060508(R) (2004).
[8] A. Damascelli *et al.*, Phys. Rev. Lett. **85**, 5194 (2000).
[9] K. M. Shen *et al.*, Phys. Rev. B **64**, 180502(R) (2001).
[10] N. Kikugawa *et al.*, Phys. Rev. B **70**, 134520 (2004).
[11] K. Hamacher, C. Gros, and W. Wenzel, Phys. Rev. Lett. **88**, 217203 (2002).
[12] S. Okamoto and A. J. Millis, Phys. Rev. B **70**, 195120 (2004).
[13] F. Lechermann, S. Biermann, and A. Georges, Phys. Rev. Lett. **94**, 166402 (2005).
[14] A. Liebsch and A. Lichtenstein, Phys. Rev. Lett. **84**, 1591 (2000).
[15] In principle, ARPES can be used to determine many-body dispersions directly. The detailed study of N. J. C. Ingle *et al.*, Phys. Rev. B **72**, 205114 (2005) concentrates on the α sheet, while H. Iwasawa *et al.*, Phys. Rev. B **72**, 104514 (2005) report dispersions for all three Fermi surface sheets, but only for $E < E_F$ and $y = 0$. Also, the masses deduced from their dispersions lead to a 35% underestimate of the specific heat for $y = 0$, for reasons which are not clear. We therefore believe that the model dispersion proposed in this Letter, which rests primarily on conclusions drawn from thermodynamic measurements, is more reliable.
[16] Band energies calculated using a tight-binding model by taking the eigenvalues (in eV) $[\epsilon'_\alpha, \epsilon'_\beta, \epsilon'_\gamma]$ of the matrix $([\alpha\beta_1, \alpha\beta_2, 0], [\alpha\beta_2, \alpha\beta_3, 0], [0, 0, \epsilon'_\gamma])$, where $\alpha\beta_1 = 0.6(-0.537 - c_y - 0.0882c_x)$, $\alpha\beta_2 = -0.174 s_x s_y$, $\alpha\beta_3 = 0.6(-0.537 - c_x - 0.0882c_y)$, and $\epsilon'_\gamma = 0.84(-0.757 - c_x - c_y - 0.832c_x c_y)$, where $c_i = \cos(k_i a)$, $s_i = \sin(k_i a)$. This improves small discrepancies between the ARPES data and the calculated γ Fermi surfaces. The resulting bandwidths are renormalized such that $E_\alpha = \epsilon'_\alpha/2.84$, $E_\beta = \epsilon'_\beta/2.56$, and $E_\gamma = \epsilon'_\gamma/6.05$.
[17] Explicit calculations of the real part of the Lindhard susceptibility from this tight-binding dispersion are shown in Refs. [6,10], following a procedure first used for bare LDA bands in Sr_2RuO_4 by I. I. Mazin and D. J. Singh, Phys. Rev. Lett. **82**, 4324 (1999).
[18] P. Monthoux and G. G. Lonzarich, Phys. Rev. B **71**, 054504 (2005).